J Appl Physiol 115: 1032–1042, 2013.
First published July 18, 2013; doi:10.1152/japplphysiol.00537.2013.

Model-based causal closed-loop approach to the estimate of baroreflex sensitivity during propofol anesthesia in patients undergoing coronary artery bypass graft

Alberto Porta,[1] Vlasta Bari,[2,3] Tito Bassani,[4] Andrea Marchi,[4] Valeria Pistuddi,[5] and Marco Ranucci[5]

[1]*Department of Biomedical Sciences for Health, Galeazzi Orthopedic Institute, University of Milan, Milan, Italy;* [2]*Gruppo Ospedaliero San Donato Foundation, Milan, Italy;* [3]*Department of Electronics Information and Bioengineering, Politecnico di Milano, Milan, Italy;* [4]*Humanitas Clinical and Research Center, Rozzano, Italy; and* [5]*Department of Anesthesia and Intensive Care, Policlinico San Donato, San Donato Milanese, Italy*

Submitted 2 May 2013; accepted in final form 13 July 2013

Porta A, Bari V, Bassani T, Marchi A, Pistuddi V, Ranucci M. Model-based causal closed-loop approach to the estimate of baroreflex sensitivity during propofol anesthesia in patients undergoing coronary artery bypass graft. *J Appl Physiol* 115: 1032–1042, 2013. First published July 18, 2013; doi:10.1152/japplphysiol.00537.2013.—Cardiac baroreflex is a fundamental component of the cardiovascular control. The continuous assessment of baroreflex sensitivity (BRS) from spontaneous heart period (HP) and systolic arterial pressure (SAP) variations during general anesthesia provides relevant information about cardiovascular regulation in physiological conditions. Unfortunately, several difficulties including unknown HP-SAP causal relations, negligible SAP changes, small BRS values, and confounding influences due to mechanical ventilation prevent BRS monitoring from HP and SAP variabilities during general anesthesia. We applied a model-based causal closed-loop approach aiming at BRS assessment during propofol anesthesia in 34 patients undergoing coronary artery bypass graft (CABG) surgery. We found the following: *1*) traditional time and frequency domain approaches (i.e., baroreflex sequence, cross-correlation, spectral, and transfer function techniques) exhibited irremediable methodological limitations preventing the assessment of the BRS decrease during propofol anesthesia; *2*) Granger causality approach proved that the methodological caveats were linked to the decreased presence of bidirectional closed-loop HP-SAP interactions and to the increased incidence of the HP-SAP uncoupling; *3*) our model-based closed-loop approach detected the significant BRS decrease during propofol anesthesia as a likely result of accounting for the influences of mechanical ventilation and causal HP-SAP interactions; and *4*) the model-based closed-loop approach found also a diminished gain of the relation from HP to SAP linked to vasodilatation and reduced ventricular contractility during propofol anesthesia. The proposed model-based causal closed-loop approach is more effective than traditional approaches in monitoring cardiovascular control during propofol anesthesia and indicates an overall depression of the HP-SAP closed-loop regulation.

blood pressure variability; heart rate variability; mechanical ventilation; autonomic nervous system; cardiovascular control; general anesthesia

BAROREFLEX SENSITIVITY (BRS) is habitually estimated by measuring the variation of the temporal distance between two consecutive QRS complexes, taken as an approximation of heart period (HP), per unit change of systolic arterial pressure (SAP) following the administration of a vasoactive drug (52). BRS significantly decreased during propofol-induced general anesthesia at high anesthetic concentration levels (23, 31, 47, 50). Several signal processing techniques have been proposed to estimate BRS without pharmacologically challenging cardiovascular control both in time and frequency domains (32). These approaches opened the possibility to continuously monitor baroreflex function through the assessment of spontaneous HP and SAP variabilities in any condition including general anesthesia (21).

Frequency domain approaches require the fulfillment of two prerequisites for the reliable estimation of BRS (17, 20): *1*) the HP-SAP correlation must be significant in the low-frequency (LF, from 0.04 to 0.15 Hz) and/or in the high-frequency (HF, from 0.15 to 0.4 Hz) bands; and *2*) HP changes must lag behind SAP variations in the same frequency bands. Time domain approaches require the fulfillment of similar prerequisites in the time domain (i.e., the normalized cross-correlation function should exhibit a significant peak, and the time shift at its occurrence should be compatible with the baroreflex latency) (26, 51, 55, 56). Usually the prerequisites for time domain approaches are checked locally over any candidate baroreflex sequence (10, 11) or any running window (55) by optimizing the lag between HP an SAP and checking the significance of their correlation. The fulfillment of both these two prerequisites should guarantee that HP and SAP variabilities are related along the time direction from SAP to HP (i.e., along cardiac baroreflex). Unfortunately, both these two conditions are inappropriate to test the involvement of baroreflex in governing HP-SAP dynamical interactions, even if checked together. Indeed, the correlation between HP and SAP variabilities might be significant even in presence of inactive baroreflex due to the strong interaction between HP and SAP along the reverse temporal direction (i.e., from HP to SAP) due to Starling law and diastolic runoff (44) leading to opposite sign changes of SAP in response to the same HP variations. The pathway from HP to SAP is frequently referred to as feedforward mechanical pathway. In addition, phase, in the case of frequency domain approaches, or lag, in the case of time domain techniques, is almost useless to infer causality in the interaction between HP and SAP series (i.e., which drives which). Indeed, in the frequency domain, negative phase shifts can be turned out into positive values (and vice versa) by arbitrary selecting phase multiple (43). On the other hand, in the time domain, temporal shift at the peak of the normalized cross-correlation function is largely biased by common rhythmical sources affecting both

Address for reprint requests and other correspondence: A. Porta, Università degli Studi di Milano, Dipartimento di Scienze Biomediche per la Salute, Istituto Ortopedico Galeazzi, Laboratorio di Modellistica di Sistemi Complessi, Via R. Galeazzi 4, 20161 Milan, Italy (e-mail: alberto.porta@unimi.it).

HP and SAP series (e.g., respiration) regardless of the causal HP-SAP interactions (26).

These methodological difficulties, operating in every experimental condition, are extremely limiting during propofol anesthesia. Indeed, because of the dramatic depression of the sympathetic activity (23, 50), SAP variability in the LF band is extremely reduced (54), thus restraining the possibility that SAP oscillations in the LF band could solicit baroreflex and drive LF oscillations of the HP series. In addition, positive pressure mechanical ventilation profoundly affects HP and SAP series by imposing strong rhythmicities on both series at the ventilatory rate (8). Although these influences determine a significant correlation between HP and SAP series at the ventilatory rate, they do not guarantee the stimulation of the baroreflex (e.g., phase shifts at the ventilatory rate incompatible with the baroreflex latency have been reported during general anesthesia) (9, 57). This difficulty might become insurmountable when assessing BRS in patients that might be characterized by a low BRS just before the induction of general anesthesia, such as those undergoing coronary artery bypass graft (CABG) surgery with a history of hypertension (39). These difficulties prevent the routine monitoring of BRS during general anesthesia, thus importantly limiting the possibility to typify cardiovascular control in this condition. Because some recent studies have suggested the link between low BRS values and major adverse cardiovascular events (12, 35), it could be hypothesized that patients who experience atrial fibrillation after cardiac surgery (20–30% of the cases) have an impaired BRS before surgery. Also, patients undergoing perioperative renal failure related to CABG might take advantage from the BRS monitoring (4). Therefore, a reliable monitoring of BRS in this setting may be useful to identify patients at risk for arrhythmias or renal failure, thus prompting for an early pharmacological treatment.

This study proposes the application of a model-based causal closed-loop approach for the assessment of BRS based on spontaneous HP and SAP variabilities (5) during general anesthesia induced by intravenous administration of propofol in patients undergoing CABG. Because this approach interprets the causal relations between HP and SAP variabilities, models the HP-SAP closed-loop interactions (i.e., the feedback pathway from SAP to HP and the feedforward pathway from HP to SAP), and accounts for the joint influences of positive pressure mechanical ventilation on both HP and SAP series, we hypothesize that it could be more effective than traditional methods, such as baroreflex sequence, cross-correlation, spectral, and transfer function methods (10, 38, 41, 45, 55), for BRS estimation during general anesthesia. The Granger causality approach, accounting explicitly for respiration, was utilized to make evident the changes in the HP-SAP causal relationships during propofol-induced general anesthesia, thus supporting the need to go beyond traditional methods with a model-based causal approach. A group of patients undergoing CABG with an history of hypertension was selected because of the low BRS in resting condition, thus making more challenging the detection of the decrease of BRS due to the induction of propofol anesthesia.

MATERIALS AND METHODS

Experimental protocol. According to the Declaration of Helsinki for medical research involving human subjects and following approval of the ethical review board of the Policlinico San Donato and signed informed consent, 34 patients (ASA III-IV; ages 50–88 yr, median 70 yr; 31 males) scheduled for CABG surgery were studied. A demographic and preoperative profile of the patient population is given in Table 1. Entry criteria were sinus rhythm, age >18 yr, and left ventricular ejection fraction ≥40%. A large percentage (79%) of these patients had a history of hypertension. We excluded patients undergoing emergency operation. Patients were studied ahead of surgery before the induction of general anesthesia (PRE) and after intubation of the trachea, during general anesthesia, before the chest was opened (POST). The PRE session was recorded after application of standard premedications including intramuscular administration of atropine (0.5 mg) and fentanyl (100 μg). Anesthesia was induced by the intravenous administration of propofol, as a hypnotic agent, and remifentanil, as analgesic. Anesthesia was induced with an intravenous bolus injection of propofol at 1.5 mg/kg and maintained with continuous infusion at 3 $mg \cdot kg^{-1} \cdot h^{-1}$. The range of administration of remifentanil was from 0.05 to 0.5 $\mu g \cdot kg^{-1} \cdot min^{-1}$ (0.32 ± 0.11 $\mu g \cdot kg^{-1} \cdot min^{-1}$, mean ± SD). The PRE session was recorded 15 min before the induction of the anesthesia. During the PRE session the subjects breathed spontaneously, whereas during the POST session they were mechanically ventilated with a rate of 12–16 breaths/min. During the POST session the patients inhaled a mixture of air and oxygen (1:1) provided by a closed breathing system (fresh gas flow of 3 l/min oxygen and 3 l/min air). Mechanical ventilation was administered according to a volume-controlled mode. The POST session was recorded when the target plasma concentration of propofol was expected to be around 3 μg/ml based on the pharmacokinetic properties of the drug. ECG from lead II and invasive arterial pressure from the radial artery were recorded using an analog-to-digital board

Table 1. *Demographic and preoperative profile of the patient population*

Variable	No. of Patients or Mean ± SD
No. of subjects	34
Sex (male)	31
Age, yr	68.7 ± 8.8
Weight, kg	73.8 ± 12.2
Obesity (body mass index >30)	4
Left ventricular ejection fraction, %	55.9 ± 10.7
Recent myocardial infarction (<30 days)	3
Unstable angina	0
Congestive heart failure	1
Serum creatinine level, mg/dl	0.97 ± 0.30
Chronic obstructive pulmonary disease	2
Previous cerebrovascular accident	1
Diabetes on medication	7
History of hypertension (AHA definition)	27
Hematocrit, %	38.5 ± 4.4
Serum bilirubin level, mg/dl	0.49 ± 0.21
Pa_{O_2} at POST recording, mmHg	126 ± 52
Pa_{CO_2} at POST recording, mmHg	34.9 ± 6.4
ACE inhibitors	27
Beta blockers	31
Calcium antagonists	8
Digitalis	0
Amiodarone	2
Furosemide	7

Values indicate either the no. of patients exhibiting the given variable or the mean ± SD of the measured variable across subjects. ACE, angiotensin converting enzyme; AHA, American Heart Association; Pa_{O_2} and Pa_{CO_2}, arterial O_2 and CO_2 partial pressure; POST, after induction of general anesthesia.

(National Instruments, Austin, TX) plugged into a laptop computer directly connected to the patient's monitor. PRE and POST sessions lasted 10 min. The signals were sampled at 250 Hz.

Extraction of the beat-to-beat variability series. After the QRS complex was detected on the ECG and the R apex located using parabolic interpolation, the temporal distance between two consecutive R parabolic apexes was computed and utilized as an approximation of HP. The maximum of arterial pressure inside HP was defined as SAP, and the *i*th SAP [i.e., SAP(i)] was taken inside the *i*th HP [i.e., HP(i)], where i is the cardiac beat counter. Respiration (R) series was obtained from the respiratory-related amplitude modulation of the ECG. The amplitude of the first QRS complex delimiting HP(i) with respect to the isoelectric line was taken as the *i*th R measure [i.e., R(i)]. The occurrences of QRS and SAP peaks were carefully checked to avoid erroneous detections or missed beats. If isolated ectopic beats affected HP and SAP values, these measures were linearly interpolated using the closest values unaffected by ectopic beats. HP(i), SAP(i) and R(i) measures were performed on a beat-to-beat basis, thus obtaining the beat-to-beat series HP = {HP(i), $i = 1, \ldots, N$}, SAP = {SAP(i), $i = 1, \ldots, N$}, and R = {R(i), $i = 1, \ldots, N$} where N is the series length. Sequences with $N = 200$ were randomly selected inside each experimental condition. The series were linearly detrended. If evident nonstationarities, such as very slow drifting of the mean or sudden changes of the variance, were visible despite the linear detrending, the random selection was carried out again. The mean and the variance of HP and SAP were indicated as μ_{HP}, μ_{SAP}, σ^2_{HP}, and σ^2_{SAP}, respectively (expressed in ms, mmHg, ms^2, and mmHg^2, respectively).

Power spectral density estimation. The power spectrum was estimated according to an univariate parametric approach fitting the series according to an autoregressive (AR) model (see APPENDIX, *AR spectral analysis* for further details) (36). AR spectral density was factorized into components, each of them characterized by a central frequency. A spectral component was labeled as LF (or HF) if its central frequency belonged to the LF (or HF) band. The LF and HF powers were defined as the sum of the powers of all LF and HF spectral components, respectively. The HF power of HP series, expressed in absolute units (ms^2) and labeled as HF_{HP}, was utilized as a marker of vagal modulation directed to the heart (3), whereas the LF power of SAP series, expressed in absolute units (mmHg^2) and labeled as LF_{SAP}, was utilized as a marker of sympathetic modulation directed to vessels (37). The power of HP and SAP series in LF and HF bands (LF_{HP} and HF_{SAP}) was calculated as well and utilized for the estimation of BRS based on spectral approach.

Frequency domain BRS assessment. Frequency domain assessment of BRS was based on spectral (38) and transfer function (40, 41) approaches. BRS based on spectral approach was grounded on the evaluation of the power spectrum of HP and SAP series and its decomposition into components. BRS was computed as the square root of the ratio of LF_{HP} to LF_{SAP}, indicated as α_{PS}(LF) in the following. Similarly, α_{PS}(HF) was defined as the square root of the ratio of HF_{HP} to HF_{SAP}.

BRS based on transfer function approach was grounded on the computation of the ratio of the HP-SAP cross-spectrum modulus to the SAP power spectrum. BRS was computed by sampling the transfer function magnitude in correspondence of the weighted average of the central frequencies of the LF and HF components found in the SAP series, where the weights were the powers of the components. BRS transfer function estimates are indicated as α_{TF}(LF) and α_{TF}(HF). By definition, α_{PS}(LF), α_{PS}(HF), α_{TF}(LF), and α_{TF}(HF) were greater than 0.

The prerequisites of high HP-SAP correlation, indicating the presence of a significant association between HP and SAP, and negative HP-SAP phase, indicating that HP changes lagged behind SAP variations, were tested according to the calculation of squared coherence ($K^2_{HP\text{-}SAP}$) and phase spectrum ($Ph_{HP\text{-}SAP}$) (20). $K^2_{HP\text{-}SAP}$ was computed as the ratio of the square cross-spectrum modulus divided by product of the power spectra of HP and SAP series, whereas $Ph_{HP\text{-}SAP}$ was the phase of the HP-SAP cross-spectrum. The cross-spectrum was estimated according to a bivariate AR model (see APPENDIX, *Bivariate AR cross-spectral analysis* for further details) (41). $K^2_{HP\text{-}SAP}$ ranged from 0 to 1, indicating a perfect uncorrelation and a full correlation, respectively. $K^2_{HP\text{-}SAP}$ and $Ph_{HP\text{-}SAP}$ were sampled in correspondence of the same LF and HF frequencies used to assess α_{TF}(LF) and α_{TF}(HF). The derived indexes were labeled as $K^2_{HP\text{-}SAP}$(LF), $K^2_{HP\text{-}SAP}$(HF), $Ph_{HP\text{-}SAP}$(LF), and $Ph_{HP\text{-}SAP}$(HF), respectively. α_{PS}(LF) and α_{TF}(LF) were calculated if the prerequisites of $K^2_{HP\text{-}SAP}(LF) > 0.5$ and $Ph_{HP\text{-}SAP}(LF) < 0$ were fulfilled. The reliable calculation of α_{PS}(HF) and α_{TF}(HF) necessitated similar requirements in the HF band. α_{PS}(LF), α_{TF}(LF), α_{PS}(HF) and α_{TF}(HF) were also computed without checking $K^2_{HP\text{-}SAP}$ and $Ph_{HP\text{-}SAP}$.

Time domain BRS assessment. Time domain assessment of BRS was based on baroreflex sequence (10) and cross-correlation (55) approaches. Baroreflex sequence technique relies on the search for sequences characterized by the contemporaneous increase (positive +/+ sequence) or decrease (negative −/− sequence) of HP and SAP. Both positive and negative sequences are referred to as baroreflex sequences. The length of the sequences was four beats (3 increases or decreases). The lag between HP and SAP values, τ, was set to 0 to pick up the fast vagal arm of the baroreflex. When plotted in the plane [SAP(i), HP($i + \tau$)], with $\tau = 0$, HP and SAP values belonging to a baroreflex sequence lay on a straight line, thus allowing a linear regression analysis. The slope of the regression line was calculated and averaged over all baroreflex sequences. This average, marked α_{SEQ} in the following, was taken as a measure of BRS in the time domain. A baroreflex sequences was considered to be meaningful if it matched the following prerequisites: *1*) the total HP variation was larger than 5 ms; *2*) the total SAP variation was larger than 1 mmHg; and *3*) the correlation coefficient in the plane [SAP(i), HP(i)] was larger than 0.85. α_{SEQ} was also computed without checking these prerequisites.

Cross-correlation approach relies on the assessment of the slope of the linear regression in the plane [SAP(i), HP($i + \tau$)], over a running window of length equal to 10 beats. The time lag, τ, was selected in the range from 0 to 5 by maximizing the correlation coefficient. The slope was considered to be meaningful if it was significantly larger than 0 with $P < 0.01$. The running window was moved by 1 beat and the assessment of the slope was repeated. The median of the distribution of the slope over the entire period of analysis was taken as the BRS estimate and indicated as α_{XBRS} in the following. α_{XBRS} was also computed without checking that the slope was significantly different from 0 (only positive values were retained).

Granger causality approach. Given the set of series Ω = {HP, SAP, R} representing the universe of knowledge utilized to describe cardiovascular system, SAP is said to Granger-cause HP if the HP dynamics can be better predicted in Ω than in Ω after exclusion of SAP (i.e., $\Omega - \{SAP\}$) (28). In other words, SAP is said to Granger-cause HP if SAP carries unique information about future behavior of HP that cannot be derived from any signal present in Ω other than SAP. Causality from HP to SAP can be simply defined by reversing the role between HP and SAP. The need for including R in the minimal set of series necessary to evaluate the HP-SAP casual relations was pointed out by Porta et al. (42): indeed, since R affects both HP and SAP (5, 48), disregarding R might lead to erroneous interpretation of HP-SAP causal relations. Granger approach to the evaluation of causality from SAP to HP was based on calculation of the mean square prediction error of HP in Ω and in $\Omega - \{SAP\}$ and on its subsequent comparison. The calculation of the mean square prediction error was carried out after estimation of the coefficients of an M-variate AR model in Ω with M = 3 and an (M − 1)-variate AR model in $\Omega - \{SAP\}$ (see APPENDIX, *M-variate AR model* for further details). The optimal model order chosen in Ω was maintained even in $\Omega - \{SAP\}$, but the coefficients of the model were estimated again. Comparison between the mean square prediction error of HP in Ω and

Table 2. *HP and SAP mean, variance, and spectral powers during PRE and POST sessions*

	PRE	POST
μ_{HP}, ms	902 (827–1031)	1120* (1041–1263)
σ^2_{HP}, ms^2	536 (192–1061)	161* (74–387)
HF_{HP}, ms^2	46.9 (12.2–161.8)	24.9 (6.6–50.0)
μ_{SAP}, mmHg	166 (144–184)	107* (92–125)
σ^2_{SAP}, mmHg^2	18.1 (11.8–25.7)	9.9* (6.7–13.7)
LF_{SAP}, mmHg^2	1.39 (0.46–3.08)	0.18* (0.10–0.44)

Values are medians, with the first quartile-to-third quartile range in parentheses. μ_{HP}, heart period (HP) mean; σ^2_{HP}, HP variance; HF_{HP}, power of HP series in the high-frequency (HF) band; μ_{SAP}, systolic arterial pressure (SAP) mean; σ^2_{SAP}, SAP variance; LF_{SAP}, power of SAP series in the low-frequency (LF) band; PRE, before induction of general anesthesia. *$P < 0.05$ vs. PRE.

in $\Omega - \{SAP\}$ was performed via the *F*-test (53). The *F* value for the assessment of causality along cardiac baroreflex from SAP to HP (i.e., $F_{HP\text{-}SAP}$) was estimated as the fractional predictability improvement of HP due to the addition of SAP in $\Omega - \{SAP\}$ multiplied by the ratio of the degrees of freedom of HP mean square prediction error in $\Omega - \{SAP\}$ on the degrees of freedom of the difference between the HP mean square prediction error in Ω and in $\Omega - \{SAP\}$ (42). If $F_{HP\text{-}SAP}$ was larger than the critical value of the *F* distribution for a given significance level (here 0.01), the null hypothesis that SAP did not Granger-cause HP was rejected and the alternative hypothesis of unidirectional causality from SAP to HP, indicated as SAP→HP in the following, was accepted (i.e., cardiac baroreflex is effective). Reversing the role of SAP and HP allowed the test of the null hypothesis that HP did not Granger-cause SAP and, whether rejected, the unidirectional causality from HP to SAP, indicated as HP→SAP in the following, was accepted. If both SAP→HP and HP→SAP were contemporaneously found, a closed-loop relation (bidirectional HP-SAP causality) could be argued and labeled as HP↔SAP in the following. If the null hypothesis that SAP did not Granger-cause HP and vice versa could not be rejected, HP and SAP were classified as uncoupled in Ω.

Closed-loop model-based estimate of the BRS and feedforward mechanical pathway gain. After identification of the coefficients of the M-variate model with $M = 3$ in $\Omega = \{HP, SAP, R\}$ (see APPENDIX, *M-variate AR model* for further details), the polynomials $A_{HP\text{-}SAP}(z)$ and $A_{SAP\text{-}HP}(z)$ described the baroreflex feedback arm, from SAP to HP, and the mechanical feedforward arm, from HP to SAP, of the HP-SAP closed-loop, respectively.

$A_{HP\text{-}SAP}(z)$ was fed by an artificial unitary ramp simulating an SAP rise, and the slope of the regression line of the HP response on time assessed over the first 15 samples (i.e., the slope of HP-SAP relationship following the simulated stimulus) was taken as BRS estimated via a model-based closed-loop approach (5). The model-based closed-loop estimate of the BRS was indicated as α_{CL} in the following. α_{CL} was larger than 0 when the response of $A_{HP\text{-}SAP}(z)$ led to an HP variation with the same sign of the SAP change as expected from a working baroreflex. α_{CL} could be even smaller than 0: it occurred when the HP variation had opposite sign of the SAP change due to non-baroreflex mechanisms.

The value of the first coefficient of $A_{SAP\text{-}HP}(z)$, indicated as $a_{SAP\text{-}HP}(1)$ in the following, was taken as an index quantifying the gain of the feedforward mechanical pathway from HP to SAP (5). The order of the polynomial $A_{SAP\text{-}HP}(z)$ was limited to 1 according to Baselli et al. (6). $a_{SAP\text{-}HP}(1)$ was larger than 0 when Starling effect prevailed over diastolic runoff (e.g., an increase of HP led to a larger stroke volume and, then, to a larger SAP at the next cardiac beat due to the Starling effect only partially offset by the decrease of arterial pressure due to the prolongation of the diastolic decay). $a_{SAP\text{-}HP}(1)$ was smaller than 0 when the diastolic runoff prevailed over Starling effect (e.g., an increase of HP led to a more prolonged diastolic decay, thus causing a decrease of the diastolic arterial pressure and a smaller SAP at the next cardiac beat only partially offset by the augmented stroke volume).

Statistical analysis. We performed the paired *t*-test to check the significance of the difference between indexes before and after the induction of anesthesia. If the normality test (Kolmogorov-Smirnov test) was not fulfilled, the Wilcoxon signed rank test was utilized. The paired *t*-test was substituted with the unpaired *t*-test when testing the prerequisites prevented the estimation of BRS during the PRE or POST session in at least one subject. If normality test was not fulfilled, the Mann-Whitney rank sum test was utilized. The χ^2 test was utilized to test the effect of anesthesia on the percentage of patients fulfilling the prerequisites for BRS calculation (McNemar's test). The same test was exploited to check the significance of the changes of the percentage of patients exhibiting a given HP-SAP causal relation. Statistical analysis was carried out using a commercial statistical program (SigmaStat, version 3.0.1, SPSS). A $P < 0.01$ was always considered significant.

RESULTS

Time and frequency domain univariate characterization of the HP and SAP series. Table 2 summarizes the results relevant to time and frequency domain univariate analysis of HP and SAP series. Whereas the HP mean (i.e., μ_{HP}) significantly increased after the induction of general anesthesia, the SAP mean (i.e., μ_{SAP}) significantly decreased. General anesthesia significantly lowered both HP and SAP variances (i.e., σ^2_{HP} and σ^2_{SAP}). In addition, general anesthesia produced a tendency toward a reduction of the HF power of HP series, HF_{HP}, although the decrease was not significant. The decrease was significant in the case of the LF power of SAP series, LF_{SAP}.

Assessing the prerequisites for BRS calculation. Table 3 summarizes the results relevant to the percentage of patients fulfilling the prerequisites for BRS calculation. As to the calculation of frequency domain indexes of BRS, before the induction of general anesthesia the percentage of patients with

Table 3. *Percentage of patients fulfilling the prerequisites for BRS calculation during PRE and POST*

	Prerequisites	PRE	POST
$\alpha_{PS}(LF)$, $\alpha_{TF}(LF)$	$K^2_{HP\text{-}SAP}(LF) > 0.5$ and $Ph_{HP\text{-}SAP}(LF) < 0$	41	0*
$\alpha_{PS}(HF)$, $\alpha_{TF}(HF)$	$K^2_{HP\text{-}SAP}(HF) > 0.5$ and $Ph_{HP\text{-}SAP}(HF)<0$	47	32
α_{SEQ}	At least 1 BRS sequence with total HP variation >5 ms, total SAP variation >1 mmHg, and correlation coefficient >0.85	91	32*
α_{XBRS}	At least 1 running window with slope in the plane [SAP(i), HP($i+\tau$)] significantly >0 with $P < 0.01$ with τ selected to maximize correlation coefficient	100	100
α_{CL}	Whiteness and pairwise uncorrelation of residuals	94	94

Values are percentages of patients fulfilling the following prerequisites for calculation of baroreflex sensitivity (BRS) during PRE and POST sessions: $\alpha_{PS}(LF)$ and $\alpha_{PS}(HF)$, BRS assessed using spectral approach in LF and HF bands; $\alpha_{TF}(LF)$ and $\alpha_{TF}(HF)$, BRS assessed using transfer function approach in LF and HF bands; α_{SEQ}, BRS assessed using baroreflex sequence technique; α_{XBRS}, BRS assessed using cross-correlation analysis; α_{CL}, BRS assessed using model-based closed-loop approach; $K^2_{HP\text{-}SAP}(LF)$ and $K^2_{HP\text{-}SAP}(HF)$, squared coherence function between HP and SAP series in LF and HF bands; $Ph_{HP\text{-}SAP}(LF)$ and $Ph_{HP\text{-}SAP}(HF)$, phase between HP and SAP series in LF and HF bands. *$P < 0.05$ vs. PRE.

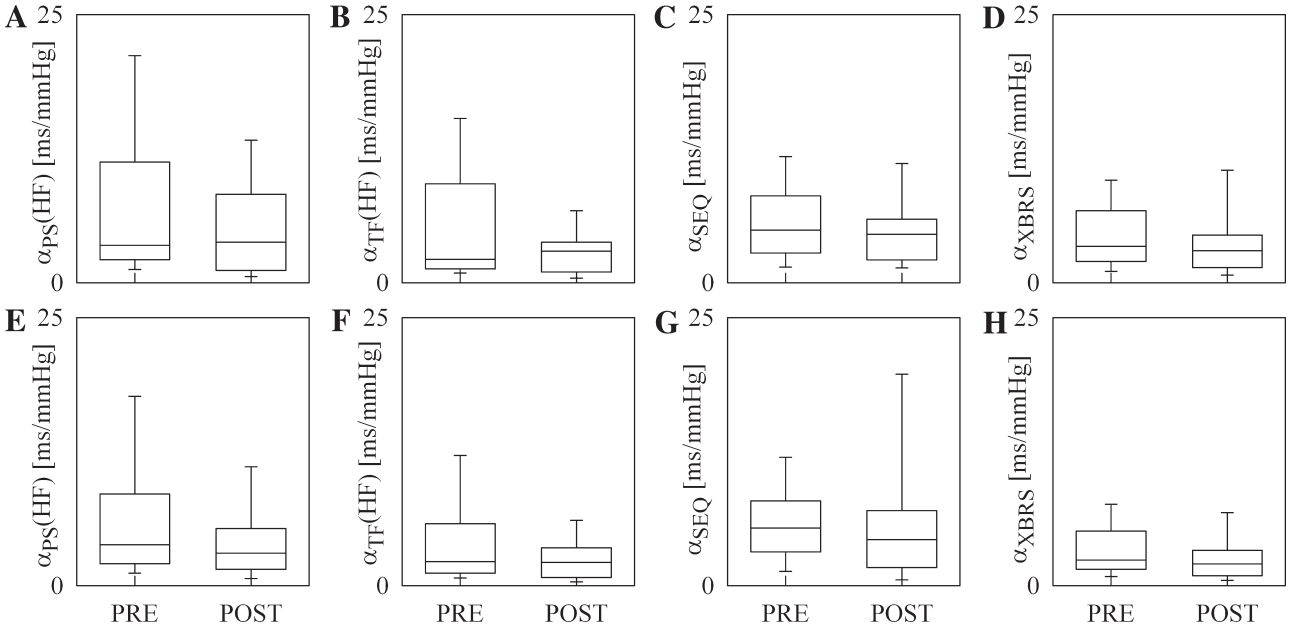

Fig. 1. Box-and-whiskers plots reporting the 10th, 25th, 50th, 75th, and 90th percentiles of the baroreflex sensitivity (BRS) assessed according to the power spectral approach in the high-frequency (HF) band, α_{PS}(HF) (A and *E*), the transfer function approach in the HF band, α_{TF}(HF) (*B* and *F*), the baroreflex sequence analysis, α_{SEQ} (*C* and *G*), and the cross-correlation technique, α_{XBRS} (D and H), before the induction of general anesthesia (PRE) and after intubation of the trachea during general anesthesia (POST). BRS indexes were computed over those subjects fulfilling the prerequisites for the analysis, as reported in Table 1 (*A–D*), and without checking the prerequisites for the analysis (*E–H*). No significant differences were detected between PRE and POST.

$K^2_{HP\text{-}SAP}(LF) > 0.5$ and $Ph_{HP\text{-}SAP}(LF) < 0$ was 41% in the case of α_{PS}(LF) and α_{TF}(LF) and 47% in the case of α_{PS}(HF) and α_{TF}(HF). After the induction of general anesthesia, this percentage remained unmodified in the case of α_{PS}(HF) and α_{TF}(HF) (i.e., 32%), whereas it dropped to 0% in the case of α_{PS}(LF) and α_{TF}(LF). This reduction was mainly due to the significant decrease of $K^2_{HP\text{-}SAP}$(LF): the median value of $K^2_{HP\text{-}SAP}$(LF) decreased from 0.36 during PRE to 0.11 during POST. As to the calculation of α_{SEQ}, before the induction of anesthesia the percentage of patients with at least one meaningful baroreflex sequence (i.e., with total HP variation >5 ms, total SAP variation >1 mmHg, and correlation coefficient >0.85) was important (i.e., 91%). This percentage significantly declined (i.e., 32%) during propofol anesthesia. As to the calculation of α_{XBRS}, at least one running window with HP-SAP slope significantly larger than 0 was found in all the patients (i.e., 100%) both before and after induction of general anesthesia. The prerequisites for the calculation of α_{CL} (i.e., whiteness and pairwise uncorrelation of the residuals) were fulfilled in 94% of the patients before propofol induction, and this percentage remained stable during general anesthesia (i.e., 94%).

BRS estimates. Figure 1 shows the results relevant to the assessment of BRS based on spectral, transfer function, baroreflex sequence, and cross-correlation analyses. The BRS assessed in LF band [i.e., α_{PS}(LF) and α_{TF}(LF)] was not plotted because after the induction of propofol anesthesia, none of the subjects had $K^2_{HP\text{-}SAP}(LF) > 0.5$ and $Ph_{HP\text{-}SAP}(LF) < 0$. When BRS indexes were computed over those subjects fulfilling the prerequisites listed in Table 3, the median of α_{PS}(HF), α_{TF}(HF), α_{SEQ}, and α_{XBRS} before the induction of general anesthesia was as low as 3.47, 2.16, 4.88, and 3.38 ms/mmHg, respectively (Fig. 1, *A–D*). Propofol anesthesia did not depress significantly these indexes (Fig. 1, *A–D*). When BRS indexes were computed without checking the prerequisites for BRS calculation [i.e., in 100, 100, 97, and 100% of the patients in the case of α_{PS}(HF), α_{TF}(HF), α_{SEQ}, and α_{XBRS}, respectively], the median of α_{PS}(HF), α_{TF}(HF), α_{SEQ}, and α_{XBRS} before the induction of anesthesia was 3.82, 2.23, 5.38, and 2.37 ms/mmHg, respectively (Fig. 1, *E–H*). Again, no statistically significant differences between PRE and POST were detected (Fig. 1, *E–H*).

Causality in HP-SAP variability interactions. Figure 2 summarizes the results of causality analysis. Before the induction of propofol anesthesia, HP and SAP series were never found to be uncoupled. They were coupled solely in the temporal direction from SAP to HP (i.e., along the cardiac baroreflex) in 12% of the patients, solely along the temporal direction from HP to SAP (i.e., along the mechanical feedforward pathway) in 32% of the patients, and in both temporal directions, indicating an active HP-SAP closed-loop relation, in 56% of the patients.

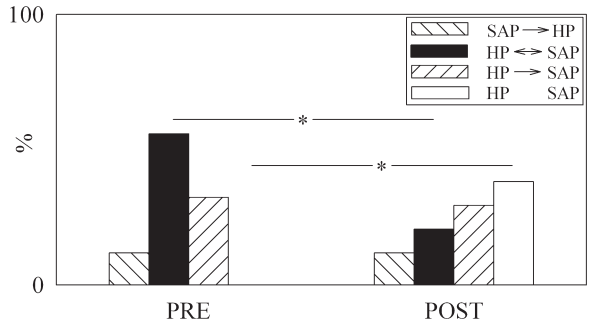

Fig. 2. Bar graph reporting the percentage of heart period (HP) and systolic arterial pressure (SAP) causal interactions during PRE and POST. The percentage of SAP→HP, HP↔SAP, HP→SAP, and uncoupled HP and SAP are shown. *$P < 0.01$ vs. PRE.

After the induction of propofol anesthesia, the percentage of subjects with closed-loop HP-SAP interactions significantly decreased to 21%, whereas the percentage of subjects exhibiting uncoupled HP and SAP dynamics significantly increased to 38%. The percentage of unidirectional interactions along cardiac baroreflex (from SAP to HP) or feedforward mechanical pathway (from HP to SAP) was not affected by propofol anesthesia.

Model-based closed-loop estimation of the gain of the baroreflex feedback and feedforward mechanical pathways. Figure 3 shows the results relevant to the gain of the relation from SAP to HP, α_{CL} (Fig. 3*A*), and from HP to SAP, $a_{SAP\text{-}HP}(1)$, assessed using the model-based closed-loop approach (Fig. 3*B*). The median values of α_{CL} and $a_{SAP\text{-}HP}(1)$ were 1.15 ms/mmHg and −24.1 mmHg/s, respectively. α_{CL} significantly diminished to 0.04 ms/mmHg after the induction of propofol anesthesia (Fig. 3*A*), thus indicating a depressed baroreflex regulation. During the POST session, $a_{SAP\text{-}HP}(1)$ became significantly less negative (i.e., −12.1 mmHg/s) and moved toward 0 (Fig. 3*B*), thus indicating a depressed response of SAP to HP variations. Taken together, both results show that the overall gain of the HP-SAP closed-loop regulation is dramatically reduced during propofol anesthesia in CABG patients.

DISCUSSION

The findings of this study can be summarized as follows: *1*) during propofol anesthesia, BRS from spontaneous HP and SAP variabilities was assessed in a negligible percentage of patients using traditional techniques with the exception of cross-correlation approach; *2*) our model-based approach accounting for HP-SAP causal interactions, closed-loop relation between HP and SAP variabilities, and influences of positive pressure mechanical ventilation on both HP and SAP allowed the measurement of the BRS in the majority of the patients during propofol anesthesia; *3*) the proposed model-based closed-loop approach detected the decrease of BRS after the induction of propofol anesthesia, whereas all the traditional methods failed; *4*) propofol anesthesia imposed a modification of the causal relations between HP and SAP series by reducing the likelihood of the closed-loop HP-SAP interactions and increasing that of HP-SAP uncoupling; *5*) the gain of the mechanical feedforward pathway was significantly reduced, thus indicating a diminished effect of HP changes on SAP attributable to vasodilatation and reduction of ventricular contractility induced by propofol administration; and *6*) the decrease of the gain of the baroreflex feedback and of the mechanical feedforward pathways suggests the overall depression of the HP-SAP regulation during propofol anesthesia.

HP and SAP variabilities during propofol anesthesia. It is well known that propofol anesthesia is characterized by hypotension in humans (18, 54). This finding was also confirmed in animals (2, 46). Our time domain parameters corroborated the vasodilatation effects of propofol. The bradycardic response of propofol, observed in humans (18, 19) and animals (2, 46), is more controversial, because several studies were not able to detect it (29, 34, 47), whereas others observed a tachycardic response in the first minutes after the induction of anesthesia (23, 50). In this study we found a significant bradycardia may be partially related to the choice of recording the PRE session, just before the induction of the anesthesia, with the patients that, although quiet, have been waiting for a cardiac surgery. Also, premedications might have influenced baseline values of variables during the PRE session, even though they should not have played a role in setting the difference between PRE and POST sessions. It was also reported that the amount of HP variability, quantified by the HP variance, significantly went down, and the relevant decrease in the HF band was interpreted as a result of the vagal withdrawal induced by anesthesia (19, 29, 34). A significant decline of the amount of SAP variability, quantified by the SAP variance, was found as well, and the dramatic drop in the LF band was correlated to the depression of sympathetic activity (54). Our time and frequency domain parameters (Table 2) confirmed all these findings, thus underlining the overall depression of the autonomic function during propofol anesthesia in patients undergoing CABG surgery.

Difficulties in estimating traditional time and frequency domain BRS indexes from HP and SAP variabilities during propofol anesthesia. The assessment of BRS based on HP and SAP spontaneous variabilities is grounded on the hypothesis of a significant involvement of baroreflex in governing HP-SAP variability interactions. This involvement is usually tested by checking the significance of the degree of association between HP and SAP series and the presence of a delayed response of HP variations to SAP changes compatible with the baroreflex latency, thus suggesting a significant causal relation along cardiac baroreflex (i.e., from SAP to HP). In the case of BRS indexes derived in the frequency domain, these prerequisites are checked according to the calculation of squared coherence and phase spectrum (17, 20, 43). These two functions are usually sampled at predefined frequencies of interest: LF and

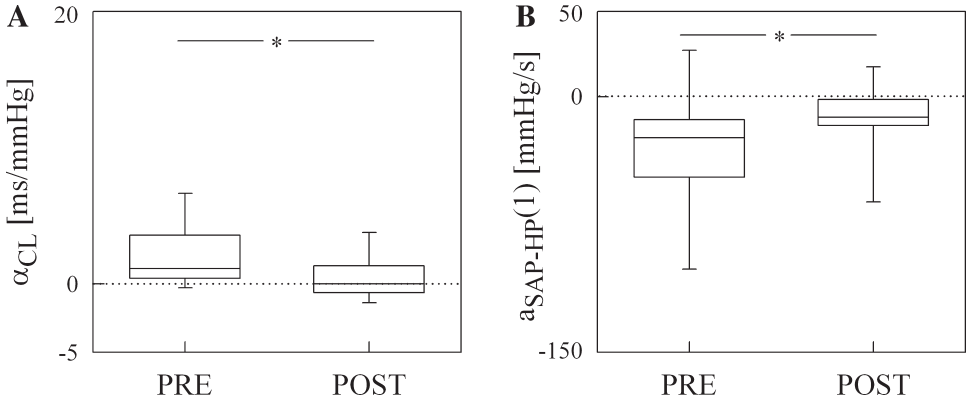

Fig. 3. Box-and-whiskers plots reporting the 10th, 25th, 50th, 75th, and 90th percentiles of the gain of the cardiac baroreflex (i.e., from SAP to HP), α_{CL} (*A*), and the gain of the mechanical feedforward pathway (i.e., from HP to SAP), $a_{SAP\text{-}HP}(1)$ (*B*), assessed according to the model-based causal closed-loop approach during PRE and POST. $*P <$ 0.01 vs. PRE.

HF are traditionally selected given the importance of these rhythmicities in short-term cardiovascular control (20, 36). By convention it is assumed that whether squared coherence at the frequency of interest is larger than 0.5, the HP and SAP variabilities are significantly coupled at that frequency (20), even though a more precise computation of the threshold to reject the null hypothesis of HP-SAP uncoupling is based on the construction of a set of uncoupled isospectral isodistribution surrogate series (11, 27, 44). By convention it is assumed that if phase at the frequency of interest is compatible with a delayed response of HP changes to SAP variations (i.e., negative values with the convention for cross-spectrum calculation utilized in this study), causality is from SAP to HP at that frequency (17, 20, 43). Because this prerequisite is more likely to be fulfilled in the LF band than in the HF one (25, 43), the assessment of BRS is usually recommended in LF band (33). In the case of time domain parameters similar prerequisites are checked without any a priori definition of the frequencies of interest. This check involves the computation of the normalized cross-correlation function and the assessment of its peak value at a time lag compatible with a lagged response of HP to SAP changes. This check is performed locally on every candidate baroreflex sequence and on every short time window in the case of the baroreflex sequence method and the cross-correlation technique, respectively, and the lag from SAP to HP is usually chosen as the one maximizing cross-correlation function (10, 11, 41, 55, 56). Given the small magnitude of the LF oscillations of SAP during propofol anesthesia, it is not surprising to find out that the HP-SAP squared coherence is below the threshold of significance in all the patients. This prevents the estimation of the BRS in the LF band (i.e., the band where the baroreflex is more likely to be active) during propofol anesthesia in patients undergoing CABG surgery. The finding is in disagreement with Chen et al. (13), reporting a significant squared coherence during propofol anesthesia. This disagreement might be related to the different population (i.e., healthy young volunteers vs. patients undergoing CABG surgery) and to the different level of target propofol concentration (i.e., 1 vs. 3 μg/ml). During anesthesia the squared coherence in the HF band was significantly larger than in the LF band, but a considerable amount of patients with high squared coherence had phase values incompatible with the baroreflex latency. This finding is not surprising during positive pressure mechanical ventilation: indeed, phase values incompatible with the baroreflex latency have been observed during propofol anesthesia in animals (9) and humans (57). This finding is quite common even in healthy subjects during spontaneous breathing and led to the acknowledgment of a possible non-baroreflex-mediated origin of the respiratory sinus arrhythmia, probably related to the direct coupling between respiratory centers and vagal outflow (25). Therefore, even in the HF band, the percentage of CABG patients exhibiting significant squared coherence and phase compatible with the baroreflex latency during propofol anesthesia was quite low (i.e., 32%), thus limiting the possibility to infer BRS from spontaneous variability in the frequency domain. Similar disappointing results were obtained in the time domain by exploiting baroreflex sequence analysis (10). Indeed, during propofol anesthesia a vast majority of the candidate baroreflex sequences did not fulfill the prerequisites for being selected as meaningful due to the lack of a significant correlation between HP and SAP values. As a result, only 32% of the patients during propofol anesthesia exhibited at least one meaningful baroreflex sequence. Only the cross-correlation technique (55) led to the estimation of BRS in 100% of the patients before and after induction of general anesthesia. These remarkable difficulties in fulfilling the assumptions for a reliable estimation of BRS during propofol anesthesia led some researchers to give up the exploitation of spontaneous HP and SAP variabilities and to stimulate directly carotid baroreceptors via a neck chamber device at a preselected frequency (31) to induce a measurable HP variability linked to baroreflex activity.

Causal relations between HP and SAP variability during propofol anesthesia. The above-described difficulties during propofol anesthesia in patients undergoing CABG surgery can be ascribed to the significant change of causality occurring after the induction of general anesthesia compared with the baseline condition. Indeed, before the induction of anesthesia, the most common causal relation was the bidirectional closed-loop one, whereas during propofol anesthesia, the HP and SAP series were frequently uncoupled. The percentage of patients in which the baroreflex was solicited (i.e., the sum of the percentage of patients with bidirectional closed-loop HP-SAP causality and with unidirectional causality from SAP to HP) was 68% before the induction of anesthesia and dropped to 32% after the administration of propofol. This result is in disagreement with Dorantes Mendez et al. (22), reporting 100% of bidirectional closed-loop HP-SAP causality during propofol anesthesia. This disagreement might be related to the inclusion of the respiratory signal in the set of signals utilized to interpret causal relations among HP and SAP series. Indeed, it was demonstrated (42) that respiration is a latent confounder for the causality analysis. In other words, if respiration is not accounted for, as in Dorantes Mendez et al. (22), the direct influences of respiration over HP and SAP series might be erroneously attributed to the closed-loop interactions between HP and SAP series, thus overestimating the role played by baroreflex in governing HP-SAP variability interactions. This bias of causality analysis was significant both in experimental conditions characterized by spontaneous breathing (42) and under positive pressure mechanical ventilation during general anesthesia (8). The small percentage of patients with a significant causal relation from SAP to HP can be taken as a further proof of the depression of baroreflex control during propofol anesthesia.

Effect of propofol anesthesia on BRS indexes derived from HP and SAP variabilities. The consequence of the above-mentioned limitations of traditional time and frequency domain indexes for the BRS estimation from spontaneous HP and SAP fluctuations was the inability to detect the expected decrease of BRS during propofol anesthesia (23, 31, 47, 50). The difficulties of traditional techniques were likely to be amplified by the selected group of subjects enrolled for the study (i.e., patients undergoing CABG surgery with a history of hypertension). Indeed, when α_{PS}, α_{TF}, α_{SEQ}, and α_{XBRS} were assessed over those subjects fulfilling the assumptions for their reliable quantification, very low BRS values were computed even before the induction of anesthesia (i.e., 3.47, 2.16, 4.88, and 3.38 ms/mmHg, respectively). These small BRS values increased the corruptive influence of noise on the BRS estimate. It is remarkable that BRS values assessed without checking the prerequisites

for their reliable calculation are similar to those computed according to the reliability criteria, thus suggesting that prerequisites are useless in limiting the effects of biasing sources in this experimental protocol, probably in connection with the roughness of the model underpinning traditional techniques. Conversely, the proposed model-based causal closed-loop approach was able to detect the decrease of BRS after the induction of propofol anesthesia. This success could be attributed to the ability of the method to account for HP-SAP causality and explicitly model the influences of positive pressure mechanical ventilation on both HP and SAP variabilities, thus possibly limiting the effects of biasing sources.

Closed-loop model-based approach detected the decrease of the gain of the feedforward mechanical pathway. One of the major advantages of the proposed model-based approach, in addition to the ones related to the interpretation of casual relations between HP and SAP variabilities and of the influences of mechanical ventilation on both HP and SAP series, is the possibility to quantify the gain of the relation from HP to SAP (i.e., the mechanical feedforward pathway). The gain was assessed as the coefficient of the link from HP($i - 1$) to SAP(i) [i.e., $a_{SAP\text{-}HP}(1)$] (5, 6). $a_{SAP\text{-}HP}(1)$ was the balance of two opposite effects of HP on SAP: *1*) a positive effect (i.e., the SAP increase at the next cardiac cycle occurring in response to a longer HP) caused by a more important stretching of the ventricular fibers during a longer diastolic time, and *2*) a negative effect (i.e., the SAP decrease at the next cardiac cycle occurring in response to a longer HP) caused by a lower diastolic pressure due to a longer diastolic runoff in the presence of an unchanged pulse pressure. In this study $a_{SAP\text{-}HP}(1)$ was negative in 88% of the patients before the induction of anesthesia. This result suggests that the negative effect is dominant before the induction of anesthesia (5). Given the important bradycardia and vasodilatation after the induction of propofol anesthesia, an additional increase of HP should not contribute further to the reduction of arterial pressure via diastolic decay. Conversely, as a result of an important Starling effect, a positive influence of HP on SAP is expected, thus leading to $a_{SAP\text{-}HP}(1)$ significantly larger than 0. In contrast with the expectations, $a_{SAP\text{-}HP}(1)$ was negative in 76% of the patients after the induction of propofol anesthesia. This result might be the result of the decrease of left ventricular contractility occurring during propofol anesthesia (46). The significant trend of $a_{SAP\text{-}HP}(1)$ toward 0 [i.e., $a_{SAP\text{-}HP}(1)$ became significantly less negative], thus indicating that HP variations produced less remarkable SAP changes, substantiates further the depression of left ventricular contractility imposed by the administration of propofol (23, 46). It is worth stressing that a reduced vascular reactivity to endogenous catecholamines and/or an increased vascular compliance also might play a role in determining the observed trend of $a_{SAP\text{-}HP}(1)$. However, to distinguish among these different alternatives it would be necessary to render the model more complex by accounting for the beat-to-beat series of peripheral resistance and vascular compliance.

Limitations of the study. Although BRS values were small compared with those estimated using the transfer function approach in healthy young subjects in supine resting condition (17) and in line with those derived from hypertensive patients the day before elective surgery (39), thus supporting the difficulty of the task, this smallness was not verified by comparing BRS estimates assessed from spontaneous variabilities with BRS estimated using more conventional techniques. Future studies pointing in this direction might be helpful to evaluate the level of agreement between conventional and variability-based techniques during general anesthesia. Interpretation of the findings of spectral analysis are based on the assumption that LF power of the SAP series expressed in absolute units is a marker of sympathetic modulation directed to vessels, usually holding in more standard experimental conditions. Future studies should be planned to test this assumption, for example, by correlating beat-to-beat fluctuations of muscle nerve sympathetic activity with SAP variability in the LF band (37) during general anesthesia. This limitation should have limited effect on the discussion of BRS estimates because findings are almost exclusively related to the HF band. Because the study did not make use of devices monitoring the depth of anesthesia, a certain amount of variability of the indexes during the POST session might be the consequence of different depth of anesthesia. We cannot exclude the possibility that the standardization of the depth of the anesthesia might lead to increase the statistical power of the BRS indexes, thus observing more easily significant differences between PRE and POST.

Perspective and significance. The study proposed a model-based causal closed-loop approach to the BRS assessment from spontaneous HP and SAP variabilities overcoming the limitations of spectral, transfer function, baroreflex sequence, and cross-correlation techniques. This approach was applied to an experimental condition characterized by the depression of baroreflex control, the profound modification of the HP-SAP causal relation, and the dominant influences of mechanical ventilation of both HP and SAP variabilities (i.e., during general anesthesia). At difference with traditional BRS approaches, model-based causal closed-loop technique allowed the estimation of the BRS during anesthesia in the majority of the patients, even though the considered group had very low BRS values just before the induction of anesthesia. Therefore, we conclude that the proposed approach might be worth being applied to monitor BRS during general anesthesia. In addition, it allows the estimation of gain of the relation from HP to SAP (i.e., the gain of the mechanical feedforward pathway) as well, thus completing the description of the closed-loop HP-SAP regulation during general anesthesia. This method could be a valuable tool to better understand differences among anesthesiological strategies (i.e., intravenous vs. volatile) (14), to compare different drugs within the same anesthesiological strategy (halothane vs. sevoflurane) (16), to contrast different modalities of mechanical ventilation (pressure controlled vs. pressure support mechanical ventilation) (9), to manage the increased arterial pressure lability observed upon the emergence from general anesthesia (15), and to improve perioperative risk models (4). Also, critical care medicine might take advantage for a more reliable continuous monitoring of BRS. The full exploitation of this approach might improve the management of patients during general anesthesia and reduce the incidence of postoperative adverse major cardiac events.

APPENDIX

AR spectral analysis. The variations of HP, SAP, and R about their mean values were modeled as an AR model (36). The AR model describes the dynamics as a linear combination of p past samples weighted by constant coefficients plus a zero mean white noise. The Levinson-Durbin recursive algorithm was utilized to estimate directly from the data the coefficients of the AR model and the variance of the white noise. The number of coefficients p was chosen according to the Akaike's figure of merit in the range from 14 to 18. Power spectral density was computed from the AR coefficients and from the variance of the white noise according to the maximum entropy spectral estimation approach (30). The power spectral density was factorized into a sum of terms, referred to as spectral components, the sum of which provides the entire power spectral density (58). Power spectral decomposition provided the central frequency of the components expressed in cycles per beats. It was converted into Hz by dividing the values by μ_{HP}.

Bivariate AR cross-spectral analysis. The dynamics of HP and SAP series about their mean values were jointly described as a bivariate AR model (41).The bivariate AR model describes the dynamics of the output series as a linear combination of p past samples of the same series and p past samples of the other series (considered as input) weighted by the constant coefficients plus a zero mean white noise, where p is the model order of the bivariate process. HP-SAP cross-spectrum and HP and SAP autospectra were computed from the coefficients of the bivariate AR model and from the variance of the white noises as in Porta et al. (44). The model order was fixed to 10, and the coefficients of the bivariate AR model were identified via a least-squares approach (7).

M-variate AR model. The dynamics of M series, $y_1, y_2, \ldots, y_M$, about their mean values in $\Omega = \{y_1, y_2, \ldots, y_M\}$ can be jointly described as an M-variate AR process (53). The M-variate AR model describes the dynamics of y_m, with $1 \leq m \leq M$, in Ω as the sum of an AR contribution of y_m and $M - 1$ exogenous contributions of y_j, with $1 \leq j \leq M$ and $j \neq m$,

$$y_m(i) = \sum_{j=1}^{M} A_{m,j}(z) \cdot y_j(i) + w_m(i), \qquad (1)$$

where $A_{m,j}(z) \cdot y_j(i)$ represents the linear combination of samples of y_j weighted by constant coefficients describing the dependence of y_m on y_j with $1 \leq j \leq M$ and w_m is a white noise describing the random, unpredictable part of the dynamics of y_m in Ω. The pathway from y_j to y_m is described by the transfer function

$$A_{m.j}(z) = \sum_{k=\tau_{m,j}}^{p} a_{m,j}(k) \cdot z^{-k}, \qquad (2)$$

where $a_{m,j}(k)$ is the constant coefficient linking $y_j(i - k)$ to $y_m(i)$, z^{-1} is the unit delay operator in the z domain [i.e., $z^{-1}y_j(i) = y_j(i - 1)$], p is the model order, and $\tau_{m,j}$ is the delay from y_j to y_m. $A_{m,j}(z)$ can be assessed in the frequency domain by evaluating z along the unit circle in the complex plane (i.e., $z = e^{j2\pi fT}$ with $T = \mu_{HP}$ expressed in s). If $j = m$, $\tau_{m,j} = 1$ and $A_{m,j} \cdot (z)y_m(i)$ is composed by p terms. If $j \neq m$, $\tau_{m,j}$ might be equal to 0 if immediate influences of y_j on y_m are supposed to be present or larger than 0 in the presence of lagged effects. In the present application, immediate interactions were taken into account from SAP to HP and from R to HP (i.e., $\tau_{HP,SAP} = 0$ and $\tau_{HP,R} = 0$), thus allowing the description of the fast vagal reflex (within the same cardiac beat) capable of modifying HP in response to changes of SAP and R (24, 41), and from R to SAP (i.e., $\tau_{SAP,R} = 0$), to account for the rapid effect of R on SAP due to the immediate transfer of an alteration of intrathoracic pressure on SAP value (5). Conversely, $\tau_{SAP,HP} = 1$ described the one-beat delayed effect of HP on SAP due to the measurement conventions preventing HP(i) from modifying SAP(i) (5). According to Saul et al. (48, 49), actions of HP and SAP on R are slower (i.e., they cannot occur in the same beat), thus leading to $\tau_{R,HP} = 1$ and $\tau_{R,SAP} = 1$. All the coefficients of $A_{m,j}(z)$, $a_{m,j}(k)$, were identified in Ω directly from the series using a traditional least-squares approach and the Cholesky decomposition method (7, 53). The model order, p, was optimized in the range from 4 to 16 according to the Akaike figure of merit for multivariate processes (1). The prediction of $y_m(i)$, $\hat{y}_m(i)$, can be calculated as (53)

$$\hat{y}_m(i) = \sum_{j=1}^{M} \hat{A}_{m,j}(z) \cdot y_j(i), \qquad (3)$$

where $\hat{A}_{m,j}(z)$ is the polynomial $A_{m,j}(z)$ with the estimated coefficients $\hat{a}_{m,j}(k)$ with $\tau_{m,j} \leq k \leq p$. By defining the prediction error of $y_m(i)$, $e_m(i)$, as the difference between $y_m(i)$ and $\hat{y}_m(i)$, the mean square prediction error divided by the variance of y_m can be calculated. It is commonly taken as a normalized measure of predictability of y_m in Ω (i.e., the closer to 0 the value, the better the prediction; the closer to 1 the value, the worse the prediction). The model structure is deemed to be suitable for describing interactions of series in Ω if all the residuals, e_m, in Ω are white and uncorrelated each other, even at zero lag. The whiteness of e_m and their pairwise uncorrelation, even at zero lag, were verified as in Porta et al. (41).

DISCLOSURES

No conflicts of interest, financial or otherwise, are declared by the authors.

AUTHOR CONTRIBUTIONS

A.P. and M.R. conception and design of research; A.P., V.B., T.B., and A.M. analyzed data; A.P. and M.R. interpreted results of experiments; A.P., V.B., and T.B. prepared figures; A.P. drafted manuscript; A.P., V.B., and M.R. edited and revised manuscript; A.P., V.B., T.B., A.M., and M.R. approved final version of manuscript; V.B., V.P., and M.R. performed experiments.

REFERENCES

1. **Akaike H.** A new look at the statistical novel identification. *IEEE Trans Automat Contr* 19: 716–723, 1974.
2. **Akine A, Suzuka H, Hayashida Y, Kato Y.** Effects of ketamine and propofol on autonomic cardiovascular function in chronically instrumented rats. *Auton Neurosci* 87: 201–208, 2001.
3. **Akselrod S, Gordon D, Ubel FA, Shannon DC, Berger RD, Cohen RJ.** Power spectrum analysis of heart rate fluctuations: a quantitative probe of beat-to-beat cardiovascular control. *Science* 213: 220–223, 1981.
4. **Aronson S, Fontes ML, Miao Y, Mangano DT.** Risk index for perioperative renal dysfunction/failure. Critical dependence on pulse pressure hypertension. *Circulation* 115: 733–742, 2007.
5. **Baselli G, Cerutti S, Badilini F, Biancardi L, Porta A, Pagani M, Lombardi F, Rimoldi O, Furlan R, Malliani A.** Model for the assessment of heart period and arterial pressure variability interactions and respiratory influences. *Med Biol Eng Comput* 32: 143–152, 1994.
6. **Baselli G, Cerutti S, Civardi S, Malliani A, Pagani M.** Cardiovascular variability signals: towards the identification of a closed-loop model of the neural control mechanisms. *IEEE Trans Biomed Eng* 35: 1033–1046, 1988.
7. **Baselli G, Porta A, Rimoldi O, Pagani M, Cerutti S.** Spectral decomposition in multichannel recordings based on multivariate parametric identification. *IEEE Trans Biomed Eng* 44: 1092–1101, 1997.
8. **Bassani T, Bari V, Marchi A, Wu MA, Baselli G, Citerio G, Beda A, Gama de Abreu M, Güldner A, Guzzetti S, Porta A.** Coherence analysis overestimates the role of baroreflex in governing the interactions between heart period and systolic arterial pressure variabilities during general anesthesia. *Auton Neurosci-Basic Clin.* In press; DOI:10.1016/j.autneu.2013.03.007.
9. **Beda A, Güldner A, Simpson DM, Carvalho NC, Franke S, Uhlig C, Koch T, Pelosi P, Gama de Abreu M.** Effects of assisted and variable mechanical ventilation on cardiorespiratory interactions in anesthetized pigs. *Physiol Meas* 33: 503–519, 2012.
10. **Bertinieri G, di Rienzo M, Cavallazzi A, Ferrari AU, Pedotti A, Mancia G.** A new approach to analysis of the arterial baroreflex. *J Hypertens* 3: S79–S81, 1985.
11. **Blaber AP, Yamamoto Y, Hughson RL.** Methodology of spontaneous baroreflex relationship assessed by surrogate data analysis. *Am J Physiol Heart Circ Physiol* 268: H1682–H1687, 1995.

12. **Cebula S, Sredniawa B, Kowalczyk J, Musialik-Lydka A, Wozniak A, Sedkowska A, Swiatkowski A, Kalarus Z.** The significance of heart rate turbulence in predicting major cardiovascular events in patients after myocardial infarction treated invasively. *Ann Noninvasive Electrocardiol* 17: 230–240, 2012.
13. **Chen Z, Purdon PL, Harrell G, Pierce ET, Walsh J, Brown EN, Barbieri R.** Dynamic assessment of baroreflex control of heart rate during induction of propofol anesthesia using a point process method. *Ann Biomed Eng* 39: 260–276, 2011.
14. **Citerio G, Franzosi MG, Latini R, Masson S, Barlera S, Guzzetti S, Pesenti A.** Anaesthesiological strategies in elective craniotomy: randomized, equivalence, open trial–The NeuroMorpfeo trial. *Trials* 10: 19, 2009.
15. **Cividjian A, Rentero N, Pequignot JM, Quintin L.** Effect of catecholamine depletion on increased blood pressure lability upon emergence from halothane anesthesia in rats. *J Anesth* 22: 140–148, 2008.
16. **Constant I, Laude D, Hentzgen E, Murat I.** Does halothane really preserve cardiac baroreflex better than sevoflurane? A noninvasive study of spontaneous baroreflex in children anesthetized with sevoflurane versus halothane. *Anesth Analg* 99: 360–369, 2004.
17. **Cooke WH, Hoag JB, Crossman AA, Kuusela TA, Tahvanainen KU, Eckberg DL.** Human responses to upright tilt: a window on central autonomic integration. *J Physiol* 517: 617–628, 1999.
18. **Cullen PM, Turtle M, Prys-Roberts C, Way WL, Dye J.** Effect of propofol anesthesia on baroreflex activity in humans. *Anesth Analg* 66: 1115–1120, 1987.
19. **Dautschman CS, Harris AP, Fleisher LA.** Changes in heart rate variability under propofol anesthesia: a possible explanation for propofol-induced bradycardia. *Anesth Analg* 79: 373–377, 1994.
20. **De Boer RW, Karemaker JM, Strackee J.** Relationships between short-term blood pressure fluctuations and heart rate variability in resting subjects. I: A spectral analysis approach. *Med Biol Eng Comput* 23: 352–358, 1985.
21. **di Rienzo M, Castiglioni P, Mancia G, Pedotti A, Parati G.** Advancements in estimating baroreflex function. *IEEE Eng Med Biol Mag* 2: 25–32, 2001.
22. **Dorantes Mendez GD, Aletti F, Toschi N, Canichella A, Dauri M, Coniglione F, Guerrisi M, Signorini MG, Cerutti S, Ferrario M.** Baroreflex sensitivity variations in response to propofol anesthesia: comparison between normotensive and hypertensive patients. *J Clin Monit Comput* 27: 417–426, 2013.
23. **Ebert TJ, Muzi M, Berens R, Goff D, Kampine JP.** Sympathetic responses to induction of anesthesia in humans with propofol or etomidate. *Anesthesiology* 76: 725–733, 1992.
24. **Eckberg DL.** Temporal response patterns of the human sinus node to brief carotid baroreceptor stimuli. *J Physiol* 258: 769–782, 1976.
25. **Eckberg DL, Karemaker JM.** Respiratory sinus arrhythmia is due to a central mechanism vs. respiratory sinus arrhythmia is due to the baroreflex mechanism. *J Appl Physiol* 106: 1740–1744, 2009.
26. **Faes L, Nollo G, Porta A.** Mechanisms of causal interaction between short-term RR interval and systolic arterial pressure oscillations during orthostatic challenge. *J Appl Physiol* 114: 1657–1667, 2013.
27. **Faes L, Pinna GD, Porta A, Maestri R, Nollo G.** Surrogate data analysis for assessing the significance of the coherence function. *IEEE Trans Biomed Eng* 51: 1156–1166, 2004.
28. **Granger CW.** Testing for causality. A personal viewpoint. *J Econ Dyn Control* 2: 329–352, 1980.
29. **Kanaya N, Hirata N, Kurosawa S, Nakayama M, Namiki A.** Differential effects of propofol and sevoflurane on heart rate variability. *Anesthesiology* 98: 34–40, 2003.
30. **Kay SM, Marple SL.** Spectrum analysis: a modern perspective. *Proc IEEE* 69: 1380–1418, 1981.
31. **Keyl C, Schneider A, Dambacher M, Wegenhorst U, Ingenlath M, Gruber M, Bernardi L.** Dynamic cardiocirculatory control during propofol anesthesia in mechanically ventilated patients. *Anesth Analg* 91: 1188–1195, 2000.
32. **Laude D, Elghozi JL, Girard A, Bellard F, Bouhaddi M, Castiglioni P, Cerutti C, Cividjian A, di Rienzo M, Fortrat JO, Janssen B, Karemaker JM, Leftheriotis G, Parati G, Persson PB, Porta A, Quintin L, Regnard J, Rudiger H, Stauss HM.** Comparison of various techniques used to estimate spontaneous baroreflex sensitivity (the EuroBaVar study). *Am J Physiol Regul Integr Comp Physiol* 286: R226–R231, 2004.
33. **Lipman RD, Salisbury JK, Taylor JA.** Spontaneous indexes are inconsistent with arterial baroreflex gain. *Hypertension* 42: 481–487, 2003.
34. **Maenpaa M, Penttila J, Laitio T, Kaisti K, Kuusela T, Hinkka S, Scheinin H.** The effects of surgical levels of sevoflurane and propofol anaesthesia on heart rate variability. *Eur J Anaesthesiol* 24: 626–633, 2007.
35. **Okada N, Takahashi N, Yufu K, Murozono Y, Wakisaka O, Shinohara T, Anan F, Nakagawa M, Hara M, Saikawa T, Yoshimatsu H.** Baroreflex sensitivity predicts cardiovascular events in patients with type 2 diabetes mellitus without structural heart disease. *Circ J* 74: 1379–1383, 2010.
36. **Pagani M, Lombardi F, Guzzetti S, Rimoldi O, Furlan R, Pizzinelli P, Sandrone G, Malfatto G, Dell'Orto S, Piccaluga E, Turiel M, Baselli G, Cerutti S, Malliani A.** Power spectral analysis of heart rate and arterial pressure variabilities as a marker of sympatho-vagal interaction in man and conscious dog. *Circ Res* 59: 178–193, 1986.
37. **Pagani M, Montano N, Porta A, Malliani A, Abboud FM, Birkett C, Somers VK.** Relationship between spectral components of cardiovascular variabilities and direct measures of muscle sympathetic nerve activity in humans. *Circulation* 95: 1441–1448, 1997.
38. **Pagani M, Somers VK, Furlan R, Dell'Orto S, Conway J, Baselli G, Cerutti S, Sleight P, Malliani A.** Changes in autonomic regulation induced by physical training in mild hypertension. *Hypertension* 12: 600–610, 1988.
39. **Parlow JL, Bégou G, Sagnard P, Cottet-Emard JM, Levrron JC, Annat G, Bonnet F, Ghignone M, Hughson R, Viale JP, Quintin L.** Cardiac baroreflex during the postoperative period in patients with hypertension–effect of clonidine. *Anesthesiology* 90: 681–692, 1999.
40. **Pinna GD, Maestri R, Raczak G, La Rovere MT.** Measuring baroreflex sensitivity from the gain function between arterial pressure and heart period. *Clin Sci (Lond)* 103: 81–88, 2002.
41. **Porta A, Baselli G, Rimoldi O, Malliani A, Pagani M.** Assessing baroreflex gain from spontaneous variability in conscious dogs: role of causality and respiration. *Am J Physiol Heart Circ Physiol* 279: H2558–H2567, 2000.
42. **Porta A, Bassani T, Bari V, Pinna GD, Maestri R, Guzzetti S.** Accounting for respiration is necessary to reliably infer Granger causality from cardiovascular variability series. *IEEE Trans Biomed Eng* 59: 832–841, 2012.
43. **Porta A, Catai AM, Takahashi AC, Magagnin V, Bassani T, Tobaldini E, van de Borne P, Montano N.** Causal relationships between heart period and systolic arterial pressure during graded head-up tilt. *Am J Physiol Regul Integr Comp Physiol* 300: R378–R386, 2011.
44. **Porta A, Furlan R, Rimoldi O, Pagani M, Malliani A, van de Borne P.** Quantifying the strength of the linear causal coupling in closed loop interacting cardiovascular variability signals. *Biol Cybern* 86: 241–251, 2002.
45. **Robbe HW, Mulder LJ, Ruddel H, Langewitz WA, Veldman JB, Mulder G.** Assessment of baroreceptor reflex sensitivity by means of spectral analysis. *Hypertension* 10: 538–543, 1987.
46. **Royse CF, Liew DF, Wright CE, Royse AG, Angus JA.** Persistent depression of contractility and vasodilatation with propofol but not with sevoflurane or desflurane in rabbits. *Anesthesiology* 108: 87–93, 2008.
47. **Sato M, Tanaka M, Umehara S, Nishikawa T.** Baroreflex control of heart rate during and after propofol infusion in humans. *Br J Anaesth* 94: 577–581, 2005.
48. **Saul JP, Berger RD, Albrecht P, Stein SP, Chen MH, Cohen RJ.** Transfer function analysis of the circulation: unique insights into cardiovascular regulation. *Am J Physiol Heart Circ Physiol* 261: H1231–H1245, 1991.
49. **Saul JP, Berger RD, Chen MH, Cohen RJ.** Transfer function analysis of autonomic regulation. II. Respiratory sinus arrhythmia. *Am J Physiol Heart Circ Physiol* 256: H153–H161, 1989.
50. **Sellgren J, Ejnell H, Elan M, Ponten J, Wallin BG.** Sympathetic muscle nerve activity, peripheral blood flows and baroreceptor reflexes in humans during propofol anesthesia and surgery. *Anesthesiology* 80: 534–544, 1994.
51. **Silvani A, Grimaldi D, Vandi S, Barletta G, Vetrugno R, Provini F, Pierangeli G, Berteotti C, Montagna P, Zoccoli G, Cortelli P.** Sleep-dependent changes in the coupling between heart period and blood pressure in human subjects. *Am J Physiol Regul Integr Comp Physiol* 294: R1686–R1692, 2008.
52. **Smyth HS, Sleight P, Pickering GW.** Reflex regulation of the arterial pressure during sleep in man. A quantitative method of assessing baroreflex sensitivity. *Circ Res* 24: 109–121, 1969.

53. **Soderstrom T, Stoica P.** *System Identification*. Englewood Cliffs, NJ: Prentice Hall, 1988.
54. **Wang H, Kuo TB, Chan SH, Tsai TH, Lee TK, Lui PW.** Spectral analysis of arterial pressure variability during induction of propofol anesthesia. *Anesth Analg* 82: 914–919, 1996.
55. **Westerhof BE, Gisolf J, Stok WJ, Wesseling KH, Karemaker JM.** Time-domain cross-correlation baroreflex sensitivity: performance on the EUROBAVAR data set. *J Hypertens* 22: 1371–1380, 2004.
56. **Westerhof BE, Gisolf J, Karemaker JM, Wesseling KH, Secher NH, van Lieshout JJ.** Time course analysis of baroreflex sensitivity during postural stress. *Am J Physiol Heart Circ Physiol* 291: H2864–H2874, 2006.
57. **Yli-Hankala A, Porkkala T, Kaukinen S, Hakkinen V, Jantti V.** Respiratory sinus arrhythmia is reversed during positive pressure ventilation. *Acta Physiol Scand* 141: 399–407, 1991.
58. **Zetterberg LH.** Estimation of parameters for a linear difference equation with application to EEG analysis. *Math Biosci* 5: 227–275, 1969.